

# Learning The Likelihood Test With One-Class Classifiers for Physical Layer Authentication

Francesco Ardizzon, *Member, IEEE* and Stefano Tomasin, *Senior Member, IEEE*

**Abstract**—In physical layer authentication (PLA) mechanisms, a verifier decides whether a received message has been transmitted by a legitimate user or an intruder, according to some features of the physical channel over which the message traveled. To design the authentication check implemented at the verifier, typically either the statistics or a dataset of features are available for the channel from the legitimate user, while no information is available when under attack. When the statistics are known, a well-known good solution is the likelihood test (LT). When a dataset is available, the decision problem is one-class classification (OCC) and a good understanding of the machine learning (ML) techniques used for its solution is important to ensure security. Thus, in this paper, we aim at obtaining ML PLA verifiers that operate as the LT. We show how to do it with the neural network (NN) and the one-class least-squares support vector machine (OCLSSVM) models, trained as two-class classifiers on the single-class dataset and an artificial dataset. The artificial dataset for the negative class is obtained by generating channel feature (CF) vectors uniformly distributed over the domain of the legitimate class dataset. We also derive a modified stochastic gradient descent (SGD) algorithm that trains a PLA verifier operating as LT without the need for the artificial dataset. Furthermore, we show that the one-class least-squares support vector machine with suitable kernels operates as the LT at convergence. Lastly, we show that the widely used autoencoder classifier generally does not provide the LT. Numerical results are provided considering PLA on both wireless and underwater acoustic channels.

**Index Terms**—Authentication, Likelihood test, One-class classification, One-class support vector machine, Physical-layer security.

## I. INTRODUCTION

Authentication mechanisms allow a verifier, namely Bob, to check whether a received message comes from a legitimate user, Alice, or an intruder, Trudy, impersonating Alice. In physical layer authentication (PLA) schemes, the verifier extracts some channel features (CFs) (i.e., the channel impulse response or the signal attenuation) from the received signal at the physical layer and checks if they are consistent with the same CFs observed in previously received authentic messages. This solution is a valid alternative to cryptography-based authentication. The latter indeed provides authentication but is often computationally demanding and may add overhead on the transmission, therefore it is not suitable for applications with limitations on the devices' energy consumption or where the channel rate between the legitimate users is already low.

This work is supported by the project ISP5G+ ( CUP D33C22001300002), which is part of the SERICS program (PE00000014) under the NRRP MUR program funded by the EU-NGEU. The authors are with the Department of Information Engineering, Università degli Studi di Padova, Padua 35131, Italy. S. Tomasin is also with the National Inter-University Consortium for Telecommunications (CNIT), 43124 Parma, Italy. email:(francesco.ardizzon, stefano.tomasin)@unipd.it.

Depending on the information available to the verifier, two main frameworks have been investigated to decide the signal authenticity. The *statistical framework* assumes that the probability density function (pdf), or probability mass distribution (pmd), of the CFs under one or both the alternative cases (authentic or not message) is available to design a *statistical test*; the two alternatives are called *hypotheses* and the PLA verification problem is called *hypothesis testing*, [1, Ch. 6]. More recently, a *machine learning (ML) framework* has been explored, where the decision is made by a *model* that has been trained on a *dataset* of labeled CF vectors obtained under one or both alternative cases; the decision alternatives are now denoted *classes* and the PLA verification problem *classification* [2, Ch. 5].

In typical PLA scenarios (e.g., in wireless transmissions) the verifier knows the CF statistics or can collect CF vectors under legitimate conditions, i.e., for the *null hypothesis* or the *positive class*, in the statistical and ML frameworks, respectively. However, the verifier typically knows little or nothing about the intruder and thus has no pdf (or dataset) for the observations in the *alternative hypothesis* (or *negative class*). In fact, the intruder is playing against the verifier and typically can take advantage of any assumption by the verifier, choosing a different strategy. Finally, we can estimate the pdf of the CFs under attack from some past estimated channels; however, the intruder can also choose an alternative pdfs for his attack: the first is intended to induce a specific decision process, and the latter to avoid detection with the induced decision process.

In the statistical framework, without knowledge of the pdf of the CF under attack, the resulting PLA verification problem is called an *null hypothesis testing problem*. In the ML framework without a dataset from one class, we have the *one-class classification (OCC) problem*. In the statistical framework, the null hypothesis testing is based on the likelihood test (LT) that compares the probability of the CF under verification with a suitably chosen threshold. In the ML framework, several OCC solutions have been studied (see Section II for a detailed review), with the most relevant being the one-class support vector machine (OSVM) and the autoencoder (AE).

In this paper, we aim to obtain OCC methods that work as null-hypothesis testing methods to be applied in a PLA context. In particular, we aim at replicating the behavior of the LT with OCC models for PLA. Indeed, knowing the behavior of a security ML solution (thus *explaining* the model) helps in better understanding its potentials and limits for the security application, also in unpredicted situations.

We then design ML PLA models that, after appropriate learning, operate as the LT, i.e., they make the same decisions.

In particular, we consider multilayer perceptron neural network (NN) and least-square support vector machine (SVM) (SVM) [3] models. We exploit existing results showing that NNs and LS-SVM converge to the likelihood ratio test (LRT) when two labeled datasets are available. Therefore, we propose to generate an artificial dataset containing random CF vectors uniformly distributed in the domain of CF vectors from the dataset of legitimate CF (positive class), to train the NN or the LS-SVM. We also derive a modified stochastic gradient descent (SGD) algorithm to train the NN without the artificial dataset, and the resulting model will still operate as the LT at convergence. Note that the artificial dataset is used only for training, while CF provided to the OCC at exploitation can come from any distribution of the intruder CFs. We also prove that a classifier based on the AE does not provide the LT. Note that in this paper we do not present OCCs with improved performance, but classifiers that converge to the LT, which, in turn, is known to be optimal only under certain conditions. Thus, we do not compare our solution to the state-of-the-art of OCC.

In summary, the main contributions of this paper are as follows:

- We train ML models for PLA that operate as the LT, obtaining a correspondence between statistical and ML frameworks. Such models are NN and LS-SVM, trained with an artificial dataset containing random CF vectors, uniformly distributed in the domain of the target CF class.
- We provide a modified SGD algorithm for the training of a NN that does not require the generation of the artificial dataset, and we prove its convergence.
- We prove that the proposed solutions based on NN and LS-SVM converge to LT for sufficiently complex enough models and a sufficiently large target-class training set.
- We prove that a one-class least-squares support vector machine (OCLSSVM) with suitable kernels and a large-enough target-class training operates as the LT at convergence.
- We show that, in general, the AE does not provide the LT.

The rest of the paper is organized as follows. Section II presents the related state of the art and our contribution. Section III describes the PLA verification problem, analyzing it from both the ML and the statistical decision theory perspectives. Section IV introduces the LT and the proposed learning strategy for NN and OCLSSVM. In Section VI, we focus on two PLA contexts, i.e., radio transmissions and underwater acoustic communications, and we present the performance results also compared with the LT and the AE. We also consider the application of OCLSSVM on quantized channel features. Finally, Section VII gives the conclusions.

## II. RELATED LITERATURE AND MAIN CONTRIBUTIONS

PLA is based on the verification of CFs estimated from the received signal, to establish that it comes from the same transmitter as previous authentic messages. Such an approach has been widely investigated for wireless transmissions (see surveys [4], [5]) but also in other communication contexts,

such as underwater acoustic communications, e.g., in [6]–[8]. In any case, the user is identified by the CF, for instance, extracted from the impulse or frequency response such as the root mean square (RMS) delay or average tap power. Next, various tests have been proposed to assess authenticity, either based on statistics or on ML.

In the statistical framework, when the pdfs (or pmfs) of the CFs belonging to both hypotheses are known, the LRT provides the minimum misdetection (MD) probability for a given false alarm (FA) probability, as shown in the Neyman and Pearson theorem [9]. When the pdf of the CFs depends on unknown parameters under one or both hypotheses, a widely used test is the generalized likelihood ratio test (GLRT) [1]. However, the hypothesis testing problem where the pdf is completely unknown under one hypothesis is not much studied. In a similar problem, denoted universal outlier hypothesis testing [10] aims to detect the subset of  $s$  anomalous observations in a set of  $n$  observations. In both the GLRT and the universal outlier hypothesis testing, one or more CF vectors from the unknown distributions are assumed to be available, and the missing pdf (or its missing parameters) are estimated. LRT has been scarcely adopted for PLA, due to its strong assumption on the intruder behavior [11], [12], while GLRT has been considered in many papers, including [6], [13]–[16]. To the best of the authors' knowledge, the universal outlier detection was not considered until now for PLA.

When the statistical distribution is not known, but datasets of CFs are available, ML solutions should be considered. For two-class classification, when labeled datasets from both classes are available during training, supervised training for classification can be applied to several models, including (deep) NN and SVM. In [17] NNs and LS-SVMs were shown to operate as the LRT when the training dataset is large enough and the models are complex enough. In [18], the relation between statistical and ML models in PLA has been investigated. However, the authors limited the analysis to the two-class classification case, i.e., where the knowledge of either statistical descriptions or a dataset is available at Bob.

When CF vectors are available from only one class, the OCC problem arises, and typical models are the AE [19] and the OSVM [20]. Several variations of such approaches have been considered. In [21], the input data is embedded in the dissimilarity space and then represented by weighted Euclidean graphs, which are used to compute the entropy of the data distribution in the dissimilarity space and obtain decision regions. In [22], it is observed that the mean square error (MSE) loss function for the training of OSVM is robust to the Gaussian noise but less effective against large outliers, and a robust maximum correntropy loss function is proposed. In particular in [23], a OSVM combined with K-means clustering is used for PLA to verify the authenticity of an unmanned aerial vehicle used as a relay in a wireless system. A Gaussian mixture model (GMM)-based predictor is used to track the channel evolution for PLA in [24]. In [8] the authors used a recurrent NN to authenticate a moving device by observing the feature evolution of an underwater acoustic channel. Finally, an AE-based classifier is proposed in [25] to tackle the OCC problem of device fingerprinting in Wi-Fi. For

surveys on techniques for OCC, see also [19], [26], [27].

Artificial datasets for training classification models have already been considered in the literature, however under different assumptions and with different generation techniques. In [28], a two-class classifier is used for OCC, where the dataset for the negative class is randomly generated with the *same* distribution as the available dataset, obtained with a pdf estimation technique. Instead, we consider a *uniform* distribution to train a classifier equivalent to the LT. In [29], some CF vectors of the available dataset are considered to belong to the negative class, and the CF vectors that have the worst fit to the one-class model are given to an expert for labeling and then used for two-class training. We do not assume any prior knowledge of the statistical distribution nor the availability of CF vectors from the negative class. In [30], when the negative class is described by a pdf with unknown parameters, it is proposed to create a dataset for the two classes in binary classification (or classification with unknown parameters), instead of computing the LRT or GLRT: in that paper, the equivalence between GLRT and the ML techniques is supported only by a simulation campaign. In our paper instead, we assume no knowledge of the statistical distribution of the negative class (and no availability of dataset) and prove that under certain conditions the models converge to the LT. In [31], an AE is used to extract the features of the positive class, then a zero-mean Gaussian noise is applied in the latent space to generate CF vectors of the negative class; datasets are then used to train an NN. The generation of the artificial dataset is different from our approach, as we aim to obtain the LT. Finally, generative models (see the survey [26]) also include the generation of artificial datasets. In such approaches, two models are trained, the *discriminator* and the *generator*: the discriminator aims at distinguishing inputs belonging to the positive class from other inputs, while the generator aims at generating random CF vectors that fed to the discriminator are accepted as belonging to the positive class. Even in this case, the obtained solution has not been proved to be equivalent to the LT.

### III. PLA VERIFICATION PROBLEM

Consider a scenario where the legitimate transmitter Alice and the malicious transmitter (intruder) Trudy, are connected to receiver Bob, also the verifier, via a communication channel. Bob estimates CF of the channel over which signals are received. In particular, Bob estimates a CF vector  $\mathbf{x} = [x_1, \dots, x_M]^T$ , where  $T$  denotes the transpose operator, and elements  $x_j \in \mathbb{R}$ ,  $j = 1, \dots, M$ , are real numbers<sup>1</sup>. Examples of CFs are the received signal strength indicator, the angle of arrival, and the Doppler shifts [15], [27]. The CF vectors belong to a domain  $\mathcal{X} \subseteq \mathbb{R}^M$ , where  $\mathcal{X}$  is also the domain of the pdfs. We the CF vector is associated to the legitimate channel, it has pdf  $\{p_0(\mathbf{a})\}$ , while when the intruder is transmitting, the vector CF has pdf  $\{p_1(\mathbf{a})\}$ , with  $\mathbf{a} \in \mathcal{X}$ . When generated according to  $\{p_0(\mathbf{a})\}$ , we write  $\mathbf{x} \sim \mathcal{H}_0$ .

<sup>1</sup>Here we consider real-valued vectors, but other cases can be easily accommodated in the same framework, e.g., when the vector elements are discrete or complex.

When  $\mathbf{x}$  is generated from  $\{p_1(\mathbf{a})\}$ , we write  $\mathbf{x} \sim \mathcal{H}_1$ . Note that Trudy can also pre-code its signal to induce a different estimate of the CF, and we assume here that the pdf  $\{p_1(\mathbf{a})\}$  includes the effects of this precoding (see [32] and the attack strategies described therein).

The PLA verification is the problem of deciding from which pdf, and thus channel, the CF vector has been generated, i.e., designing

$$f(\mathbf{x}) \in \{\mathcal{H}_0, \mathcal{H}_1\}, \quad (1)$$

where  $f(\cdot)$  is a deterministic transformation better detailed in the following. We assume either to either know  $p_0(\cdot)$  (*statistical framework*) or have a dataset of CFs with this pdf (*ML framework*); the pdf  $p_1(\cdot)$  is instead totally unknown, as it is associated to the strategy employed by Trudy.

#### A. Non-Separability and Decision Errors

As we mentioned, in typical PLA scenarios, any same CF vector can be observed in both classes with non-zero probability. In fact, typically the CF vector is affected by estimation errors that make the CF random, under both legitimate and attack conditions. Still, we assume that pdfs  $\{p_0(\mathbf{a})\}$  and  $\{p_1(\mathbf{a})\}$  are different, thus there exists at least one CF vector which can be extracted from both Alice and Trudy channels with non-null probability. In the ML framework, this condition is denoted as *non-separability* of the two classes.

Due to non-separability, the authentication decision is not always correct, as either FA or MD errors may occur. An FA occurs a message from Alice is rejected as non-authentic, i.e.,  $f(\mathbf{x}) = \mathcal{H}_1$  while  $\mathbf{x} \sim \mathcal{H}_0$ . Similarly, an MD occurs when a message from Trudy is accepted as authentic, i.e.,  $f(\mathbf{x}) = \mathcal{H}_0$ , while  $\mathbf{x} \sim \mathcal{H}_1$ . The corresponding FA and MD probabilities are

$$\begin{aligned} P_{\text{FA}}(f) &= \mathbb{P}[f(\mathbf{x}) = \mathcal{H}_1 | \mathbf{x} \sim \mathcal{H}_0] \\ &= \int_{\mathbf{a}: f(\mathbf{a}) = \mathcal{H}_1} p_0(\mathbf{a}) d\mathbf{a}, \end{aligned} \quad (2)$$

$$\begin{aligned} P_{\text{MD}}(f) &= \mathbb{P}[f(\mathbf{x}) = \mathcal{H}_0 | \mathbf{x} \sim \mathcal{H}_1] \\ &= \int_{\mathbf{a}: f(\mathbf{a}) = \mathcal{H}_0} p_1(\mathbf{a}) d\mathbf{a}, \end{aligned} \quad (3)$$

where we have highlighted the dependency of both probabilities on the classifier or test function  $f(\mathbf{x})$ . Therefore, when designing  $f(\cdot)$  both probabilities should be considered, as discussed in the following.

In the rest of this Section, we describe the design of  $f(\mathbf{x})$  in both frameworks. In all cases, in the end, they will both compare a real value  $u$ , obtained from the CF vector  $\mathbf{x}$ , with a suitable threshold  $\delta$ . To this end, we introduce the decision function

$$\Delta(u, \delta) = \begin{cases} \mathcal{H}_0 & u > \delta, \\ \mathcal{H}_1 & u \leq \delta. \end{cases} \quad (4)$$

Threshold  $\delta$  is typically chosen to provide a desired FA probability.

### B. LT in the Statistical Framework

In the statistical framework, we say that CF vector  $\mathbf{x}$  belongs to one of two *hypotheses*: when  $\mathbf{x} \sim \mathcal{H}_0$ , the CF vector belongs to the *null hypothesis* while when  $\mathbf{x} \sim \mathcal{H}_1$ , the CF vector belongs to the *alternative hypothesis*. In this framework,  $f(\mathbf{x})$  is the *test function*. As we know only  $p_0(\cdot)$ , we resort to the LT to make the decision. In particular,

$$f_{\text{LT}}(\mathbf{x}) = \Delta(\log p_0(\mathbf{x})). \quad (5)$$

*LT As a GLRT With General Parametric pdfs*: We now show that the LT is a GLRT with specific assumptions on the pdf of the alternative hypothesis. Suppose that the pdf of the alternative hypothesis is parametric, i.e.,  $p_1(\mathbf{x}) = p_1(\mathbf{x}|\boldsymbol{\theta})$ , where  $\boldsymbol{\theta} \in \Theta$  is a vector of parameters, taken from a suitable set. Considering for example a mixture pdf with a large number of components, e.g., a GMM or a kernel density estimation (KDE), such parametric pdf can well approximate a wide set of pdfs. The set  $\Theta$  of possible parameters must be such that  $0 < p_1(\mathbf{x}, \boldsymbol{\theta}) < p_{\max}$  for any  $\mathbf{x}$  and  $\boldsymbol{\theta}$  so that we can define the GLRT

$$f_{\text{GLRT}}(\mathbf{x}) = \Delta \left[ \log \frac{p_0(\mathbf{x})}{\max_{\boldsymbol{\theta} \in \Theta} p_1(\mathbf{x}, \boldsymbol{\theta})}, \delta \right]. \quad (6)$$

Parametric pdfs as GMM and KDE are typically invariant to a translation of the CF vector  $\mathbf{x}$ , i.e., for any set of parameters  $\boldsymbol{\theta}$  and for any translation vector  $\mathbf{a}$ , there exists another set of parameters  $\boldsymbol{\theta}'$  such that  $p_1(\mathbf{x}, \boldsymbol{\theta}) = p_1((\mathbf{x} - \mathbf{a}), \boldsymbol{\theta}')$ , hence we have

$$\max_{\boldsymbol{\theta} \in \Theta} p_1(\mathbf{x}, \boldsymbol{\theta}) = p_{\max}, \quad \forall \mathbf{x}. \quad (7)$$

In this case, the denominator in (6) becomes a constant, and by properly adjusting the threshold  $\delta$ , the GLRT is equivalent to the LT (5).

### C. OCC in the ML Framework

In the ML framework, the PLA verification problem is denoted as OCC. We say that CF vector  $\mathbf{x}$  belongs to one of two *classes*: when  $\mathbf{x} \sim \mathcal{H}_0$ , the CF vector belongs to the *positive class* while when  $\mathbf{x} \sim \mathcal{H}_1$ , the CF vector belongs to the *negative class*. In this framework,  $f(\mathbf{x})$  is a *classifier*, with

$$f_{\text{ML}}(\mathbf{x}) = \Delta(\mu(\mathbf{x}, \mathbf{w}), \delta), \quad (8)$$

where  $\mu(\mathbf{x}, \mathbf{w})$  is a parametric *model* having as input the CF vectors  $\mathbf{x}$  and providing a soft real number  $\mu(\mathbf{x}, \mathbf{w})$ , with parameter vector  $\mathbf{w}$ . The setting of the parameters is obtained by a *training* using a dataset containing  $N_0$  correctly labeled vector CF vectors from the positive class, denoted as

$$\mathcal{D}_0 = \{\mathbf{x}_1, \dots, \mathbf{x}_{N_0}\}. \quad (9)$$

What distinguishes the various OCCs is the kind of used model  $\mu(\cdot)$  and the way it is trained, still using the dataset  $\mathcal{D}_0$ . In the following, we recall two OCC solutions, namely the AE and the OSVM.

*Autoencoder (AE) Classifier*: An AE is an unsupervised multilayer perceptron NN trained to replicate its input to the output. The AE can be decomposed into two sub-networks, the *encoder* providing an output in the *latent space*, and the *decoder*, giving as output a vector of the same size as the encoder input. The encoder NN  $f_e(\mathbf{x}, \mathbf{w}_e)$  (with parameter vector  $\mathbf{w}_e$ ) aims at projecting the  $M$ -dimensional input,  $\mathbf{x}$  into the  $K$ -dimensional latent space,  $\mathbf{y} \in \mathbb{R}^K$ , with  $K < M$ . The representation of the input in the latent space is then given as input to the decoder NN,  $f_d(\mathbf{x}, \mathbf{w}_d)$  (with parameter vector  $\mathbf{w}_d$ ), which aims at replicating the original input, computing the reconstructed vector  $\tilde{\mathbf{x}} = f_d(f_e(\mathbf{x}_n, \mathbf{w}_e), \mathbf{w}_d)$ . The AE is trained to minimize the MSE loss function, i.e.,

$$\begin{aligned} \min_{\mathbf{w}} \rho_{\text{AE}}(\mathcal{D}_0, \mathbf{w}) &= \\ &= \min_{\mathbf{w}} \frac{1}{N_0} \sum_{n=1}^{N_0} \|\mathbf{x}_n - f_d(f_e(\mathbf{x}_n, \mathbf{w}_e), \mathbf{w}_d)\|^2, \end{aligned} \quad (10)$$

where  $\mathbf{w} = [\mathbf{w}_e^T, \mathbf{w}_d^T]^T$ . We remark that the latent space typically has a smaller dimension than the input vector, i.e.,  $M > K$ . Thus, to replicate the input, the AE must learn the statistical properties of the input. More details about the AE design can be found in [2, Ch. 14].

In this framework, the model used for OCC provides as output the MSE between the input CF vector  $\mathbf{x}$  and the AE output  $\tilde{\mathbf{x}}$ , i.e.,

$$\mu_{\text{AE}}(\mathbf{x}, \mathbf{w}) = \|\mathbf{x} - \tilde{\mathbf{x}}\|^2, \quad (11)$$

which is then used in (8) to obtain the AE classifier. The idea behind the use of an AE for OCC is that, by training the NN using only the  $\mathcal{D}_0$  dataset, only input CF vectors with the same (or similar) pdf of the CF vectors in  $\mathcal{D}_0$  itself are expected to be reconstructed with low MSE during the test phase, [17], [33].

*One-Class Least-Squares Support Vector Machine (OCLSSVM) Classifier*: During training, the two-class SVM finds the boundary that better separates the CF vectors of the two classes. The OCLSSVM model instead is trained only on the  $\mathcal{D}_0$  dataset and finds the hyper-surface that best contains the CF vectors in  $\mathcal{D}_0$ . In details, consider a proper feature-space transformation function  $\phi: \mathbb{R}^M \rightarrow \mathbb{R}^P$ . Then, the OCLSSVM [3] is trained by solving the following optimization problem

$$\min_{\mathbf{w}=[\mathbf{w}', b]} \rho_{\text{OCLSSVM}}(\mathcal{D}_0, \mathbf{w}), \quad (12a)$$

$$\rho_{\text{OCLSSVM}}(\mathcal{D}_0, \mathbf{w}) = \frac{1}{2} \mathbf{w}'^T \mathbf{w}' + b + C \frac{1}{2} \sum_{n=1}^{N_0} e_n^2 \quad (12b)$$

$$e_n = -\mathbf{w}'^T \phi(\mathbf{x}_n) - b \quad n = 1, \dots, N_0,$$

where  $\mathbf{w} = [\mathbf{w}', b]$  is a parameter vector, and  $C$  is a hyper-parameter, [34].

The model used for OCC (8) in this case is

$$\mu_{\text{OCLSSVM}}(\mathbf{x}, \mathbf{w}) = \mathbf{w}'^T \phi(\mathbf{x}) + b. \quad (13)$$

Note that, set a proper threshold, (13) identifies the boundary of the positive class, CF vectors of  $\mathcal{D}_0$ , and that the shape of such boundary significantly depends on the choice of the transformation function  $\phi(\mathbf{x})$ .

#### IV. LT WITH NEURAL NETWORKS AND SUPPORT VECTOR MACHINES

We now propose models for PLA verification with suitable training that operate as the LT. To this end, we a) show how the LT can be described as a binary hypothesis test with a suitably defined pdf of the alternative hypothesis; b) define training and properly selected models to be used in the ML classifier (8) that, using the properly selected model, operates as LT.

##### A. LT as Hypothesis Tester

In the statistical framework, when both pdfs  $p_0(\cdot)$  and  $p_1(\cdot)$  are known, the uniformly most powerful test minimizing the MD probability for a given FA probability is the LRT, which first computes the log-likelihood ratio on the CF vector  $\mathbf{x}$

$$\Gamma(\mathbf{x}) = \log \frac{p_0(\mathbf{x})}{p_1(\mathbf{x})}, \quad \mathbf{x} \in \mathcal{X}, \quad (14)$$

and then performs the test by comparing  $\Gamma(\mathbf{x})$  with a threshold  $\delta$ , chosen to ensure the target FA probability, i.e.,

$$f_{\text{LRT}}(\mathbf{x}) = \Delta(\Gamma(\mathbf{x}), \delta). \quad (15)$$

Now, we cast the LT as a LRT, with a properly designed alternative hypothesis pdf, which is not the true (unknown)  $p_1(\cdot)$ . The following result links the LRT of hypothesis testing with the LT for the null hypothesis testing.

**Lemma 1.** *When the pdf of the alternative hypothesis is constant on the domain of the null hypothesis, i.e.,*

$$p_1(\mathbf{a}) = u(\mathbf{a}) = \begin{cases} \frac{1}{|\mathcal{X}|}, & \mathbf{a} \in \mathcal{X}, \\ 0, & \text{otherwise,} \end{cases} \quad (16)$$

where  $|\mathcal{X}|$  is the volume of  $\mathcal{X}$ , the LT (5) is **equivalent** to the LRT (15). This means that, for each threshold  $\delta_1$  there exists a threshold  $\delta_2$  such that

$$\Delta(\Gamma(\mathbf{x}), \delta_1) = \Delta(p_0(\mathbf{x}), \delta_2), \quad \forall \mathbf{x} \in \mathcal{X}. \quad (17)$$

*Proof:* By inserting the definition (16) of  $u(\mathbf{a})$  into the log-likelihood ratio (14), we have

$$\Gamma(\mathbf{x}) = \log |\mathcal{X}| + \log p_0(\mathbf{x}), \quad \mathbf{x} \in \mathcal{X}. \quad (18)$$

Considering the LRT of (15), from (4) we have

$$\begin{aligned} \Delta(\Gamma(\mathbf{x}), \delta) &= \begin{cases} \mathcal{H}_0 & \log |\mathcal{X}| + \log p_0(\mathbf{x}) > \delta \\ \mathcal{H}_1 & \log |\mathcal{X}| + \log p_0(\mathbf{x}) \leq \delta \end{cases} \\ &= \begin{cases} \mathcal{H}_0 & p_0(\mathbf{x}) > \exp[\delta - \log |\mathcal{X}|] \\ \mathcal{H}_1 & p_0(\mathbf{x}) \leq \exp[\delta - \log |\mathcal{X}|] \end{cases} \\ &= \Delta(p_0(\mathbf{x}), \delta'), \end{aligned} \quad (19)$$

with  $\delta' = \exp[\delta - \log |\mathcal{X}|]$ . Note that the last line of (19) is the LT (5), thus the tests are equivalent in the sense of (17). ■

Therefore, LT can also be seen as a binary hypothesis test, where the statistic of CF vectors under the alternative hypothesis is *uniform* over the null-hypothesis CF vector domain  $\mathcal{X}$ .

##### B. LT-Based OCC

Moving now to the ML framework, we consider here one-class classifiers implemented as follows.

- 1) Generate an artificial dataset

$$\mathcal{D}_1^* = \{\mathbf{v}_1, \dots, \mathbf{v}_{N^*}\} \quad (20)$$

of CF vectors randomly generated according to (16), and for this reason, we denote it with the \* mark.

- 2) Train a model  $\mu(\mathbf{x}, \mathbf{w})$  as a two-class classifier on the two-class labeled dataset of size  $N = N_0 + N_1^*$

$$\mathcal{D} = \{\mathcal{D}_0, \mathcal{D}_1^*\} = \{\mathbf{q}_1, \dots, \mathbf{q}_N\}, \quad (21)$$

with labels  $t_n = -1$  for CF vectors  $\mathbf{q}_n \in \mathcal{D}_0$  and  $t_n = 1$  for  $\mathbf{q}_n \in \mathcal{D}_1^*$ .

- 3) Use the trained model in the classifier (8) to obtain the one-class classifier.

We will show that when using the NN and the LS-SVM as models  $\mu(\mathbf{x}, \mathbf{w})$ , this approach implements the LT.

*NN Model:* For the model of the test function (8) we consider a NN  $\mu_{\text{NN}}(\mathbf{x}, \mathbf{w})$ , where  $\mathbf{w}$  is the vector of parameters of the NN. The NN is trained to minimize the loss function  $\rho_{\text{NN}}(\mathcal{D}, \mathbf{w})$ , i.e.,

$$\begin{aligned} \min_{\mathbf{w}} \rho_{\text{NN}}(\mathcal{D}, \mathbf{w}) &= \min_{\mathbf{w}} \mathbb{E}_{\mathcal{D}}[\beta_{\text{NN}}(\mathbf{q}, t, \mathbf{w})] \\ &= \min_{\mathbf{w}} \left[ \sum_{\mathbf{q} \in \mathcal{D}_0} \beta_{\text{NN}}(\mathbf{q}, 0, \mathbf{w}) + \sum_{\mathbf{q} \in \mathcal{D}_1} \beta_{\text{NN}}(\mathbf{q}, 1, \mathbf{w}) \right], \end{aligned} \quad (22)$$

where the per-CF vector loss function can be either the square error (for CF vector  $\mathbf{q}$  with label  $t$ )

$$\beta_{\text{NN}}(\mathbf{q}, t, \mathbf{w}) = |\mu_{\text{NN}}(\mathbf{q}, \mathbf{w}) - t|^2, \quad (23)$$

or the cross-entropy

$$\begin{aligned} \beta_{\text{NN}}(\mathbf{q}, t, \mathbf{w}) &= \\ &t \log \mu_{\text{NN}}(\mathbf{q}, \mathbf{w}) + (1 - t) \log[1 - \mu_{\text{NN}}(\mathbf{q}, \mathbf{w})]. \end{aligned} \quad (24)$$

*LS-SVM Model:* For the model of the test function (8) we consider now an LS-SVM model  $\mu_{\text{LS-SVM}}(\mathbf{x}, \mathbf{w})$ , i.e., an SVM trained using the least-square (LS) loss function, thus solving the optimization problem

$$\min_{\mathbf{w}=[\mathbf{w}', b]} \rho_{\text{LS-SVM}}(\mathcal{D}, \mathbf{w}) = \min_{\mathbf{w}=[\mathbf{w}', b]} \frac{1}{2} \mathbf{w}'^T \mathbf{w}' + C \frac{1}{2} \sum_{n=1}^N e_n^2, \quad (25a)$$

$$e_n = 1 - t_n[\mathbf{w}'^T \phi(\mathbf{q}_n) + b] \quad n = 1, \dots, N. \quad (25b)$$

We now show that the procedure described above with these models provides the LT.

**Theorem 1.** *Consider either a NN  $\mu_{\text{NN}}(\mathbf{x}, \mathbf{w})$  (trained with either the MSE or cross-entropy loss function) or an LS-SVM  $\mu_{\text{LS-SVM}}(\mathbf{x}, \mathbf{w})$  (trained with the LS loss function) over the two-class labeled dataset  $\mathcal{D} = \{\mathcal{D}_0, \mathcal{D}_1^*\}$ , obtained from the artificial dataset. When using such models in (8), we obtain one-class classifiers equivalent to the LT, when a) the training converges to the configuration minimizing the loss functions of the two models, and b) the NN is complex enough or the*

dataset  $\mathcal{D}_0$  is large enough, the training converges to the configuration minimizing the loss functions of the two models.

*Proof:* First, we recall the results of [17, Theorems 2 and 3]: under the hypotheses of the theorem, both the multilayer perceptron NN or the LS-SVM can converge to the global minimum thus when using either of them as a model  $\mu(\mathbf{x}, \mathbf{w})$ , function (8) implements the LRT. Then, when using the artificial dataset  $\mathcal{D}_1^*$  for the negative class, the LRT and the LT are equivalent, as proven in Lemma 1.

Leveraging on both the results, we can conclude that when using either a NN or a LS-SVM as models, the test function (8) converges to both the LRT and the LT. ■

### C. NN Training with Modified Gradient

Since the artificial dataset has a very simple pdf (uniform), we now consider an alternative approach, where we modify SGD training algorithm to incorporate the effects of the artificial dataset, without the need to explicitly generate it.

Let us define

$$\begin{aligned} F(\tilde{\mathbf{w}}) &= \mathbb{E}_{\mathcal{D}_1^*} [\nabla_{\mathbf{w}} \beta_{\text{NN}}(\mathbf{q}, 1, \mathbf{w})|_{\tilde{\mathbf{w}}}] = \\ &= \frac{1}{|\mathcal{X}|} \int_{\mathcal{X}} \nabla_{\mathbf{w}} \beta_{\text{NN}}(\mathbf{x}, 1, \mathbf{w})|_{\tilde{\mathbf{w}}} d\mathbf{x}. \end{aligned} \quad (26)$$

We note that (26) identifies the average gradient when  $\mathbf{x}$  belongs to the artificial negative class with pdf  $\{u(\mathbf{a})\}$ , described by (16). Note that function  $F(\cdot)$  depends on the *structure* of the NN as it only depends on the network parameters, and not on the dataset  $\mathcal{D}_0$ . Thus, we can compute such a function offline and store it either in a look-up table or as a model itself.

Let also define the gradient operator of the loss function with respect to the NN weights, computed in  $\mathbf{w} = \mathbf{w}_n$ , the NN parameter vector at iteration  $n$  as

$$g'(\mathbf{q}, t, \mathbf{w}) = \nabla_{\mathbf{w}} \beta_{\text{NN}}(\mathbf{q}, t, \mathbf{w})|_{\mathbf{w}_n}. \quad (27)$$

For the training of the NN we propose the modified SGD (MSGD) algorithm that, in round  $n$ ,  $n = 1, \dots, N_0$ , uses a modified gradient (with respect to the SGD), using only CF vectors from the dataset  $\mathcal{D}_0$ . In particular, the weights are updated as follows

$$\mathbf{w}_{n+1} = \mathbf{w}_n - \lambda [g'(\mathbf{q}_n, 0, \mathbf{w}_n) + F(\mathbf{w}_n)], \quad (28)$$

where  $\lambda$  is the learning rate.

Next, we prove the convergence of the MSGD algorithm, by leveraging the results of [35] on the convergence of the SGD algorithm.

**Lemma 2.** *Consider an SGD with gradient  $g'$  satisfying [35, Assumptions 1.2-1.5] and denote with  $\mathbf{w}^*$  the optimal weights minimizing  $\rho_{\text{NN}}(\mathcal{D}, \mathbf{w})$ . Then, the MSGD algorithm (28) with and a small enough learning rate  $\lambda$ , converges to the optimum, i.e., we have*

$$\lim_{n \rightarrow \infty} \mathbb{E}[\beta_{\text{NN}}(\mathbf{q}_n, t_n, \mathbf{w}_n) - \beta_{\text{NN}}(\mathbf{q}_n, t_n, \mathbf{w}^*)] = 0, \quad (29)$$

where the expectation is taken over a collection of datasets  $\mathcal{D}$  with the same statistics, with  $N_0, N_1 \rightarrow \infty$ .

*Proof:* See Appendix A. ■

In other terms, by exploiting the Lemma 2, we replicate the average behavior of the SGD update when the input belongs to the negative class, without explicitly generating the dataset. The main advantage of this approach is that we do not need to generate the artificial dataset and half iterations are needed for training, while the disadvantage is that we must obtain the multivariate function  $F(\mathbf{w})$  offline and we must compute it at each iteration of the training algorithm. Lastly, we note that if the domain  $\mathcal{X}$  changes, the average gradient  $F(\mathbf{w})$  must be recomputed accordingly.

### D. On the Domain $\mathcal{X}$

The knowledge of the domain  $\mathcal{X}$  of the artificial dataset may not be trivial to obtain.

In typical PLA contexts, the first possibility is that we know some properties of the CF vectors. For example, CF vectors obtained by digital sampling an analog signal, are typically clipped within an acquisition range.

A second possibility occurs when we know that the domain of CF vectors in the negative class is the same as those in the positive class. In this case, following the ML approach, we can *learn* the domain from the dataset  $\mathcal{D}_0$  as  $\hat{\mathcal{X}}$ . This approach works well when dataset  $\mathcal{D}_0$  covers all points of the domain, i.e., domain  $\mathcal{X}$  is a discrete set. When domain  $\mathcal{X}$  is a continuous set of points, we can interpolate CF vectors from  $\mathcal{D}_0$  to obtain a continuous domain.

A third case occurs in the absence of any knowledge of the negative class, including its domain, which is generally assumed to be different from that of the positive class. In this scenario, there are two cases to consider: a) the domain points of the positive class do not belong to the domain of the negative class, and b) the domain points of the negative class do not belong to the domain of the negative class.

Case a) is not problematic, since if we consider  $\{u(\mathbf{a})\}$  still uniform but over a larger domain, Lemma 1 still holds, and we still get a classifier equivalent to the LT. Instead, case b) is problematic because points of the negative class domain that do not belong to the positive class are not explored in the training phase, while they can occur in the training phase. Since the model has not been trained on these points, its behavior is hard to predict. In this case, we can extend the domain of the artificial dataset over which the uniform CF vectors are generated, to consider possible external points. Again, considering a larger domain for the artificial dataset even beyond the domain of the negative class does not change the resulting classifier; however, the drawbacks of the domain extensions are the need to generate a larger dataset, a slower convergence rate of the model, and a potentially more complex model (more layers and neurons) to obtain a classifier equivalent to the desired LT also for the new input points.

### E. On the AE Classifier

AE classifiers have not shown good performance [36] and several patches have been proposed. Here we confirm these deficiencies by the following result that compares the AE classifier to the LT.

**Theorem 2.** *The AE classifier is not equivalent to a LT, i.e., it will make in general different classifications for the same input.*

*Proof:* In [17] it has been proven that the AE is not equivalent to a LRT, thus being the LT a special case of LRT, we cannot implement it with an AE. ■

## V. LT AND THE ONE-CLASS LEAST SQUARE SVM

The LT can also be implemented by the OCLSSVM classifier described in Section III-C, with a suitable transformation function, as we show in the following Theorem.

**Theorem 3.** *Consider an OCLSSVM model  $\mu_{\text{OCLSSVM}}(\mathbf{x}, \mathbf{w})$  using a transformation function that maps different CF vectors of  $\mathcal{D}_0$  into orthonormal vectors, thus forming a basis of  $\mathcal{D}_0$ , as*

$$\phi^T(\mathbf{x})\phi(\mathbf{y}) = 0, \quad \forall \mathbf{x} \neq \mathbf{y}, \mathbf{x} \in \mathcal{D}_0, \mathbf{y} \in \mathcal{D}_0, \quad (30)$$

$$\|\phi(\mathbf{x})\|^2 = 1, \quad \forall \mathbf{x} \in \mathcal{D}_0. \quad (31)$$

*Training this model to the global minimum of (12) and using it in the classifier (8), provides a classifier equivalent to the LT when the positive-class dataset is large enough ( $N_0 \rightarrow \infty$ ).*

*Proof:* Proof in Appendix B. ■

As a transformation function we can for example consider the following mapping, which is appropriate when the vector CF vectors are taken from a finite set of  $L$  values, thus also during testing only CF vectors  $\tilde{\mathbf{x}}_\ell$ ,  $\ell = 1, \dots, L$ , may appear. Defining the  $L$ -size column vector  $\omega(\ell)$  with entries

$$[\omega(\ell)]_i = \begin{cases} 0 & i \neq \ell, \\ 1 & i = \ell, \end{cases} \quad (32)$$

a feature-space transformation function satisfying (30) is  $\phi(\tilde{\mathbf{x}}_\ell) = \omega(\ell)$ . In practice, this requires finding all unique CF vectors in the dataset  $\mathcal{D}_0$  and assigning them an integer  $\ell$ . With this choice of transformation, the *kernel function* computed between vectors  $\tilde{\mathbf{x}}_\ell$  and  $\tilde{\mathbf{x}}_i$  is the delta kernel (DK)

$$\mathbf{k}_{\text{DK}}(\tilde{\mathbf{x}}_\ell, \tilde{\mathbf{x}}_i) = \begin{cases} 0 & i \neq \ell, \\ 1 & i = \ell. \end{cases} \quad (33)$$

However, we should observe that the practical implementation of the hypothesis of Theorem 3, i.e., finding a basis that satisfies (30) and (31), may be difficult. The transformation function (32) strictly depends on the dataset  $\mathcal{D}_0$ . In fact, the size of vector  $\phi(\mathbf{x})$  obtained from the transformation grows with the size of the dataset.

However, we have the following result.

**Corollary 1.** *Consider the Gaussian radial basis function (RBF) having kernel function*

$$k_{\text{RBF}}(\mathbf{x}, \mathbf{y}) = e^{-\alpha \|\mathbf{x} - \mathbf{y}\|^2}. \quad (34)$$

*The OCLSSVM using this kernel provides a classifier equivalent to the LT, when  $\alpha \rightarrow \infty$  and the positive-class dataset is large enough ( $N_0 \rightarrow \infty$ ).*

*Proof:* We note that

$$k_{\text{RBF}}(\mathbf{x}, \mathbf{y}) \rightarrow \mathbf{k}_{\text{DK}}(\mathbf{x}, \mathbf{y}) \quad \text{for } \alpha \rightarrow \infty. \quad (35)$$

From Theorem 3, imposing a transformation function  $\phi(\cdot)$ , as the  $N_0$  grows, we conclude that the OCLSSVM is equivalent to the LT. ■

## A. Continuous Input Space

A continuous input space can be seen as an asymptotic condition of the finite discrete input space, with the number of different input values going to infinity. Using the kernel trick, the soft output of the OCLSSVM (13) can be rewritten as

$$\mu(\mathbf{x}, \mathbf{w}) = \sum_{n=1}^{N_0} w_n k(\mathbf{x}_n, \mathbf{x}), \quad (36)$$

which provides, from Theorem 3, an approximation of the input pdf computed in  $\mathbf{x}$ . We note that (36) is similar to the pdf estimate given by the KDE method, and the OCLSSVM kernel parameters can be optimized as those of KDE.

## VI. NUMERICAL RESULTS

In this Section, we numerically validate the equivalence of one-class classifiers with the LT for PLA. Then we show evidence that the AE classifier does not provide the LT. For the transmission, we consider two scenarios, i.e., radio communications on air or underwater acoustic communications.

### A. Channel Models

We consider the three scenarios to generate datasets of CF vectors and each is associated with a different channel model. First, we look at the attenuation measured from a typical wireless channel on air affected by additive white Gaussian noise (AWGN). Next, we consider a more complex GMM scenario which in turn can be used to model the statistical distribution of more complex CFs. For instance, we will look at features extracted from an underwater acoustic channel. Still, note that a mixture of Gaussian variables can well fit any pdf, thus this scenario can be adapted to many different PLA problems. Finally, we consider a finite input space dataset, modeling the effect of a strict quantization after the AWGN channel.

In each scenario datasets  $\mathcal{D}_0$  and  $\mathcal{D}_1^*$  are used during the training phase. For testing, the dataset  $\mathcal{T} = \{\mathcal{T}_0, \mathcal{T}_1\}$  is used, where  $\mathcal{T}_i$  is the dataset of CF vectors from class  $\mathcal{H}_i$ .

Sample vectors have  $M$  entries and are acquired by a digital system that clips entries of the vector outside of the range  $[-\zeta, \zeta]$ . thus any entry  $m$  such that  $[\mathbf{x}]_m > \zeta$  is saturated at  $\zeta$ , while entries  $[\mathbf{x}]_m < -\zeta$  are saturated at  $-\zeta$ . Let  $\mathcal{X}_S = [-\zeta, \zeta] \times \dots \times [-\zeta, \zeta]$  be the domain of the clipped vectors. Therefore, for the artificial dataset  $\mathcal{D}_1^*$ , we consider vectors with independent entries uniformly generated in the interval  $[-\zeta, \zeta]$ .

**Wireless AWGN Channel:** In the first scenario, Alice (Trudy) transmits a signal, while Bob, upon reception measures the raw channel frequency response. Next, after proper thresholding, Bob extracts the amplitude of the first  $M$  channel taps which are considered to be the CFs and collected in vector  $\mathbf{x}$ . More in detail,

- we consider the transmission of signal, from which  $M = 4$  channel tap amplitudes are measured,
- the  $M$  measurements are affected by independent AWGN,
- we assume that Alice's position is public while Bob's and Trudy's positions are secret,
- Before performing the test Bob normalizes each measurement by subtracting the mean (which is a function of the distance between Alice and Bob) and dividing by the standard deviation.

We remark that the mean attenuation can be easily computed by Bob since it is a function of the line-of-sight (LOS) path loss, which, in turn, is a function of the distance Alice-Bob. A similar model has been adopted in the context of drone authentication in [37].

After normalization,  $\mathbf{x}$  has a clipped multivariate Gaussian pdf with unitary variance per entry and independent entries, i.e., for  $i = 0$  (positive class) and 1 (negative class), entry  $j$  of CF vector  $\mathbf{x}$  has pdf

$$p_i(a_j) = \begin{cases} f_G(a_j), & a_j \in (-\zeta, \zeta), \\ \delta_D(a_j - \zeta) \int_{a \geq \zeta} f_G(a) da & a_j = \zeta, \\ \delta_D(a_j + \zeta) \int_{a \leq -\zeta} f_G(a) da & a_j = -\zeta, \\ 0, & \text{otherwise,} \end{cases} \quad (37)$$

where  $\delta_D(\cdot)$  is the Dirac delta function and

$$f_G(a) = \frac{1}{\sqrt{2\pi}} \exp\left(-\frac{|a - \gamma_i|^2}{2}\right). \quad (38)$$

Thus due to the normalization for the positive class (thus for CF vectors of datasets  $\mathcal{D}_0$  and  $\mathcal{T}_0$ ) the mean is  $\gamma_0 = 0 \cdot \mathbf{1}_4$ , (here  $\mathbf{1}_4 = [1, 1, 1, 1]^T$ ). On the other hand, we assume Trudy to be in a position such that the CF vector has again unitary variance, but mean in the test phase  $\gamma_1 = 3 \cdot \mathbf{1}_4$ .

Fig. 1 shows the sampling pdf of the first element of CF vectors, from the testing datasets  $\mathcal{T}_0$  and  $\mathcal{T}_1$ , and from the artificial dataset  $\mathcal{D}_1^*$ .

**Underwater Acoustic Channel:** We now consider a scenario where the distribution of the CFs can fit using a GMM. This is appropriate for the features of an underwater acoustic communication channel: indeed, in [7], we used GMM (through a KDE method) to model the underwater acoustic CFs extracted from the power-delay response. Fig. 3 shows an example of an experimental versus estimated GMM model considering the number of channel taps, the RMS delay, the average tap power, and the smoothed power. The experimental setting is described in detail in [6]. Another use of the GMM to fit the CFs extracted from an underwater acoustic channel can be found in [38] to model the signals' angle of arrival.

As an example, here we consider  $\mathbf{x}$  to be a mixture of  $M = 4$  multivariate Gaussian pdfs with unitary variance, different numbers of components  $\nu_i$ , means  $\{\gamma_{i,m}\}$ ,  $m = 1, \dots, \nu_i$ , and mixing probabilities  $\{q_{i,m}\}$ , i.e., entry  $j$  of CF vector  $\mathbf{x}$  has

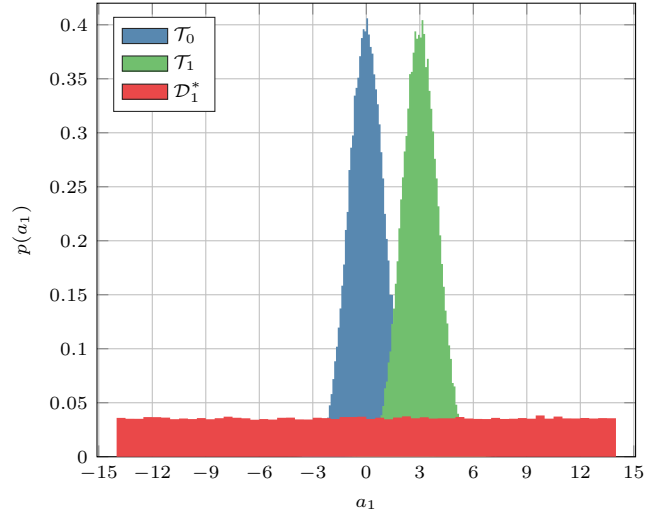


Fig. 1. Sampling pdf of the first entries of CF vectors in the datasets  $\{[\mathbf{x}]_1\}$  in the wireless AWGN Scenario: the artificially generated dataset  $\mathcal{D}_1^*$  (red) for the training phase, the  $\mathcal{T}_0$  dataset of the positive-class CF vectors (blue) for the test phase, and the  $\mathcal{T}_1$  dataset of the alternative-class CF vectors (green) for the test phase.

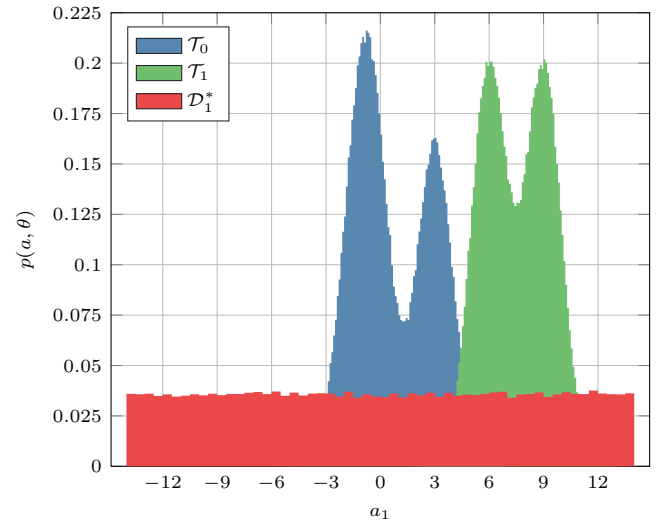


Fig. 2. Sampling pdf of the first entries of CF vectors in the datasets  $\{[\mathbf{x}_n]_1\}$  in the Mixture Scenario: the artificially generated dataset  $\mathcal{D}_1^*$  (red) for the training phase, the  $\mathcal{T}_0$  dataset of the positive-class CF vectors (blue) for the test phase, and the  $\mathcal{T}_1$  dataset of the alternative-class CF vectors (green) for the test phase.

pdf for  $i = 0$  (positive class) and 1 (negative class), entry  $j$  of CF vector  $\mathbf{x}$

$$p_i(a_j) = \begin{cases} f_M(a) & a_j \in (-\zeta, \zeta), \\ \delta_D(a_j - \zeta) \int_{a \geq \zeta} f_M(a) da & a_j = \zeta \\ \delta_D(a_j + \zeta) \int_{a \leq -\zeta} f_M(a) da & a_j = -\zeta \\ 0 & \text{otherwise,} \end{cases} \quad (39)$$

where

$$f_M(a) = \frac{1}{\sqrt{2\pi}} \sum_{m=1}^{\nu_i} q_{i,m} \exp\left(-\frac{|a - [\gamma_{i,m}]_j|^2}{2}\right). \quad (40)$$



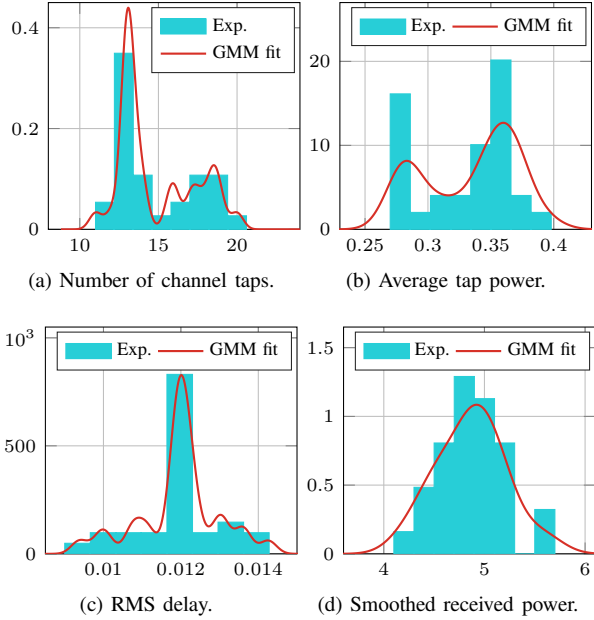


Fig. 3. Experimental (light blue) versus fitted GMM model (red).

In details, as an example, for the positive class we used  $\nu_0 = 3$  components, with probabilities  $q_{0,1} = 0.2$ ,  $q_{0,2} = 0.4$ , and  $q_{0,3} = 0.4$ , and means  $\gamma_{0,1} = -1.5 \cdot \mathbf{1}_4$ ,  $\gamma_{0,2} = -0.5 \cdot \mathbf{1}_4$ , and  $\gamma_{0,3} = 3 \cdot \mathbf{1}_4$ . For the negative class we have  $\nu_1 = 2$  components, with probabilities  $q_{1,1} = q_{1,2} = 0.5$ , and means  $\gamma_{1,1} = 6 \cdot \mathbf{1}_4$  and  $\gamma_{1,2} = 9 \cdot \mathbf{1}_4$ . Fig. 2 shows how the sampling pdf of the first element of CF vectors, from the testing datasets  $\mathcal{T}_0$  and  $\mathcal{T}_1$ , and from the artificial dataset  $\mathcal{D}_1^*$ , for the GMM Scenario.

**Finite Input Space Dataset:** We now consider a CF vector with finite entries, modeling the effect of a strict quantization after the AWGN channel. To generate  $\mathbf{x}$  we use the following procedure

- 1) We generate  $\tilde{\mathbf{x}}$  from a multivariate Gaussian with  $M = 2$ , with independent entries having pdf (38). For CF vectors generated under hypothesis 0, we have  $\gamma_0 = -1$ , while for the alternative hypothesis  $\gamma_1 = 3$ .
- 2) We quantize each entry using a 4 bit-uniform quantizer with resulting saturation region  $[-4, 8] \times [-4, 8]$ .
- 3) We randomly permute each quantized value.

Fig. 4 shows the sampling distribution of the first entry of the dataset  $\mathcal{T}_0$ , obtained as described above.

### B. Considered Solutions

For all approaches, the test phase of the PLA protocol (from which their performance is assessed) operates on a test dataset of 25000 CF vectors coming from both the positive and the negative classes. We now detail the parameters used for each classifier.

**LT-Based NN (LT-NN) Classifier:** We design the NN with 7 layers with 40, 32, 24, 16, 8, 4, and 1 neurons, respectively; all the neurons have sigmoid activation functions. The training lasted for 5 epochs; the one-class training and validation datasets have 60000 and 15000 CF vectors, respectively. The artificial dataset used for training has 60000 CF vectors.

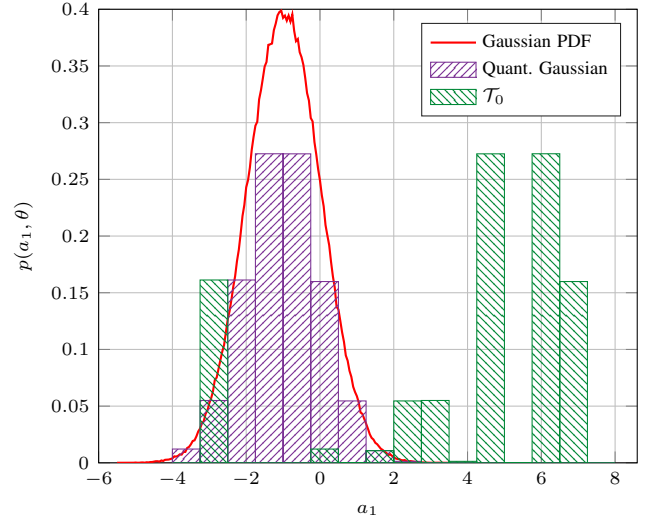


Fig. 4. Construction of the first entry of the finite input space dataset  $\mathcal{T}_0$ : original AWGN dataset pdf (red line), quantized AWGN (violet), and obtained  $\mathcal{T}_0$  pdf (green).

**LT-Based LS-SVM (LT-LS-SVM) Classifier:** As kernel function we use the RBF. Due to the computational cost of the SVM approach, we used a training dataset containing 5000 CF vectors, with  $\alpha = 2.3$ .

**One-class least-squares support vector machine (OCLSSVM) Classifier:** According to the results of Section V-A, also for the OCLSSVM we use RBF with  $\alpha = 3.4$  and the training dataset of the LT-LS-SVM classifier.

**Autoencoder (AE) Classifier:** According to the results of [39], it is not restrictive to consider a linear AEs, with 4 neurons in both input and output layers, and linear activation functions. In the hidden layer, we have instead either  $K = 1, 2$ , or 3 neurons, still with linear activation functions. Weights are initialized randomly. The model has been trained with 5 epochs and the datasets of the LT-NN classifier.

We remark that in both cases parameter  $\alpha$  was tuned by exhaustive search.

### C. Continuous Input Space

To evaluate the performance of the PLA classifiers on the continuous input spaces (Gaussian and Mixture scenarios) we consider the detection error tradeoff (DET) curves, showing the MD probability as a function of the FA probability achieved during the test phase.

**Gaussian Scenario:** Fig. 5 shows the DET for the various considered solutions in the Gaussian Scenario. We note that the LT-based classifiers perform as the LT, as expected. This occurs also for the OCLSSVM classifier, although it is not configured as in the hypotheses of Theorem 3. We also note that the AE classifier does not perform as the LT and for the considered dataset shows a worse performance. Indeed, the AE classifier performance improves as  $K$  decreases, i.e., with more compact latent space.

**Mixture Scenario:** Fig. 6 shows the DET for the PLA classifiers and the LT in the Mixture Scenario, and thus in a more complex underwater acoustic communication scenario.

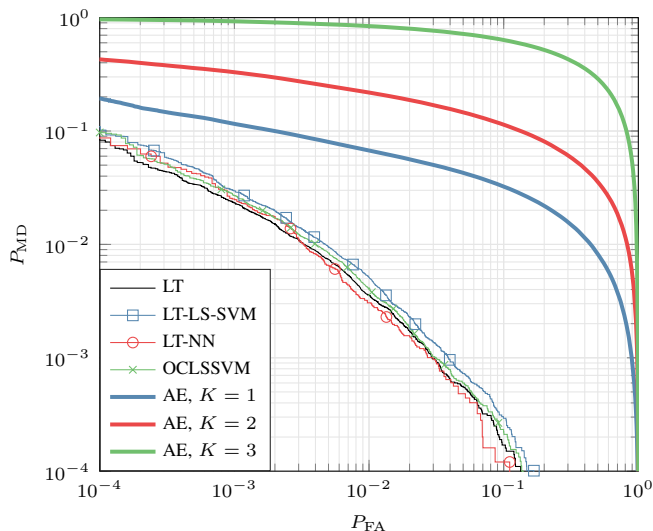


Fig. 5. DET curves for the AWGN Scenario for various classifiers and the LT.

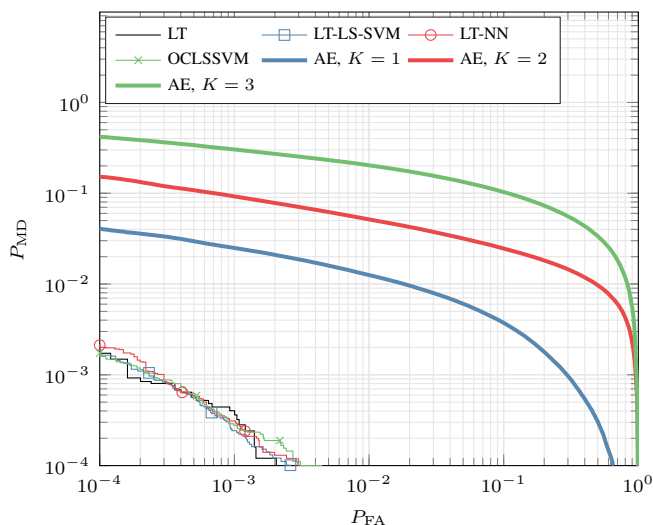


Fig. 6. DET curves for the Mixture Scenario for various classifiers and the LT.

In this case, all classifiers and the LT are better performing than in the Gaussian Scenario, due to the more marked differences between the pdfs of the CF vectors of the two classes. Also in this case, we observe that all LT-based classifiers have a similar performance and show a DET very close to that of the LT.

#### D. OCLSSVM With Finite Input Space

We now focus on the OCLSSVM and the results of Section V. A, where we considered a finite input space. First, we verify Theorem 3, showing that OCLSSVM converges to the LT when using the DK kernel (33), with a large enough training dataset. We also verify Corollary 1 by applying the RBF kernel with various values of  $\alpha$ . We consider the dataset containing CF vectors from the finite input space, described in Section VI-A.

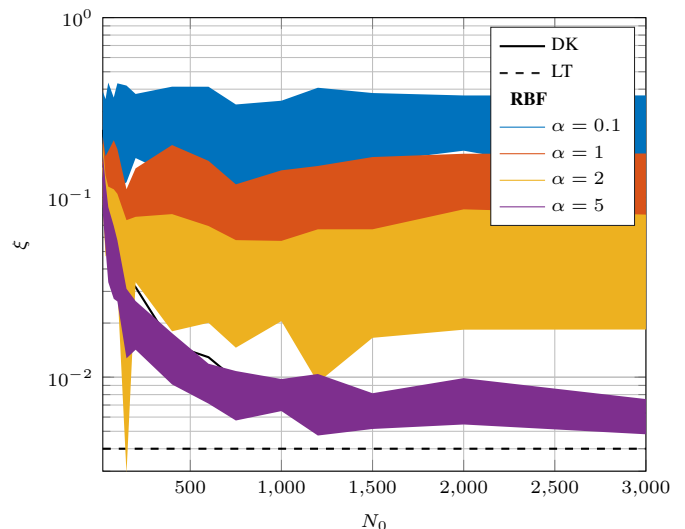


Fig. 7. Average error rate  $\xi$  as a function of  $N_0$  achieved using the OCLSSVM on the finite input space dataset, quantized with  $b = 4$  bit, and using either the RBF with  $\alpha = 0.1, 1, 2$ , and  $5$ , (colored), to the DK (black, solid), or the LT (black, dashed). Results averaged over 20 randomly generated datasets.

The performance is assessed in terms of the (average) error rate defined as

$$\xi = \frac{1}{2} \min_{\delta} (P_{FA} + P_{MD}) , \quad (41)$$

where the minimization is performed on the threshold value to make the decision.

Fig. 7 reports the average error rate  $\xi$  as a function of the training set size  $N_0$  for  $b = 4$  bit using the DK, the LT and the RBF, with  $\alpha = 0.1, 1, 2$ , and  $5$ . We remark that OCLSSVM with DK has to i) correctly identify the bases and ii) associate the weight to each basis, which in turn is related to its (estimated) probability (see (61) in the Appendix). Thus, the performance is expected to strongly depend on  $N_0$ , with high-cardinality datasets (i.e., high values of  $b$ ) requiring longer training datasets. On the other hand, for RBF with a growing  $\alpha$ , the error rate converges to the one of the LT, confirming the result of Corollary 1.

## VII. CONCLUSIONS

We considered the OCC problem in PLA aimed at identifying classifiers that learn the LT, based on the availability of only the legitimate dataset. We have identified three solutions, two are NN and SVM models trained as two-class classifiers using an artificially generated dataset, and the third is the OCLSSVM model with a proper kernel. We have investigated the conditions under which these models converge to the LT, then confirmed by numerical results on Gaussian, Gaussian mixture, and finite-space datasets, modeling respectively a wireless AWGN channel, an underwater acoustic channel, and a quantized wireless AWGN channel. Additionally, we have shown that the AE one-class classifier does not converge in general to the LT.

## REFERENCES

- [1] S. Kay, *Fundamentals Of Statistical Processing, Volume 2: Detection Theory*. Pearson Education, 2009.
- [2] I. Goodfellow, Y. Bengio, and A. Courville, *Deep Learning*. MIT Press, 2016, <http://www.deeplearningbook.org>.
- [3] Y.-S. Choi, “Least squares one-class support vector machine,” *Pattern Recognit. Lett.*, vol. 30, no. 13, pp. 1236–1240, Oct. 2009.
- [4] E. Jorswieck, S. Tomasin, and A. Sezgin, “Broadcasting into the uncertainty: Authentication and confidentiality by physical-layer processing,” *Proc. IEEE*, vol. 103, no. 10, pp. 1702–1724, Oct. 2015.
- [5] N. Xie, Z. Li, and H. Tan, “A survey of physical-layer authentication in wireless communications,” *IEEE Commun. Surv. Tutor.*, vol. 23, no. 1, pp. 282–310, Dec. 2020.
- [6] L. Bragagnolo, F. Ardizzon, N. Laurenti, P. Casari, R. Diamant, and S. Tomasin, “Authentication of underwater acoustic transmissions via machine learning techniques,” in *Proc. of COMCAS*, 2021, pp. 255–260.
- [7] F. Ardizzon, R. Diamant, P. Casari, and S. Tomasin, “Machine learning-based distributed authentication of UWAN nodes with limited shared information,” in *Proc. UComms*, 2022, pp. 1–5.
- [8] F. Ardizzon, P. Casari, and S. Tomasin, “A RNN-based approach to physical layer authentication in underwater acoustic networks with mobile devices,” *Comput. Netw.*, vol. 243, Apr. 2024.
- [9] J. Neyman and E. S. Pearson, “On the problem of the most efficient tests of statistical hypotheses,” *Philosophical Trans. of the Royal Society of London Series A*, vol. 231, pp. 289–337, Jan. 1933.
- [10] Y. Li, S. Nitinawarat, and V. V. Veeravalli, “Universal outlier hypothesis testing,” *IEEE Trans. on Info. Theory*, vol. 60, no. 7, pp. 4066–4082, Apr. 2014.
- [11] P. Zhang, T. Taleb, X. Jiang, and B. Wu, “Physical layer authentication for massive MIMO systems with hardware impairments,” *IEEE Trans. Wirel. Commun.*, vol. 19, no. 3, pp. 1563–1576, Mar. 2020.
- [12] N. Xie, M. Sha, T. Hu, and H. Tan, “Multi-user physical-layer authentication and classification,” *IEEE Trans. Wirel. Commun.*, vol. 22, no. 9, pp. 6171–6184, Sept. 2023.
- [13] P. F. Swaszek, S. A. Pratz, B. N. Arocho, K. C. Seals, and R. J. Hartnett, “GNSS spoof detection using shipboard IMU measurements,” in *Proc. of ION GNSS+*, 2014, pp. 745–758.
- [14] M. Ceccato, F. Formaggio, N. Laurenti, and S. Tomasin, “Generalized likelihood ratio test for GNSS spoofing detection in devices with IMU,” *IEEE Trans. Inf. Forensics Secur.*, vol. 16, pp. 3496–3509, May 2021.
- [15] L. Senigagliesi, G. Ciattaglia, and E. Gambi, “Autoencoder based physical layer authentication for UAV communications,” in *Proc. of Vehicular Technology Conference (VTC2023-Spring)*, 2023, pp. 1–6.
- [16] F. Ardizzon, L. Crosara, S. Tomasin, and N. Laurenti, “Enhancing spreading code signal authentication in GNSS: a GLRT-based approach,” in *Proc. of ICL-GNSS*, 2024, pp. 1–6.
- [17] A. Brighente, F. Formaggio, G. M. Di Nunzio, and S. Tomasin, “Machine learning for in-region location verification in wireless networks,” *IEEE J. Sel. Areas Commun.*, vol. 37, no. 11, pp. 2490–2502, Nov. 2019.
- [18] L. Senigagliesi, M. Baldi, and E. Gambi, “Comparison of statistical and machine learning techniques for physical layer authentication,” *IEEE Trans. Inf. Forensics Secur.*, vol. 16, pp. 1506–1521, Oct. 2021.
- [19] S. S. Khan and M. G. Madden, “One-class classification: taxonomy of study and review of techniques,” *Knowl. Eng. Rev.*, vol. 29, no. 3, pp. 345–374, June 2014.
- [20] D. M. Tax and R. P. Duin, “Data domain description using support vectors,” in *Proc. of ESANN*, vol. 99, 1999, pp. 251–256.
- [21] L. Livi, A. Sadeghian, and W. Pedrycz, “Entropic one-class classifiers,” *IEEE Trans. Neural Netw. Learn. Syst.*, vol. 26, no. 12, pp. 3187–3200, Dec. 2015.
- [22] J. Cao, H. Dai, B. Lei, C. Yin, H. Zeng, and A. Kummert, “Maximum correntropy criterion-based hierarchical one-class classification,” *IEEE Trans. Neural Netw. Learn. Syst.*, vol. 32, no. 8, pp. 3748–3754, Aug. 2021.
- [23] T. M. Hoang, N. M. Nguyen, and T. Q. Duong, “Detection of eavesdropping attack in UAV-aided wireless systems: Unsupervised learning with one-class SVM and K-means clustering,” *IEEE Wirel. Commun. Lett.*, vol. 9, no. 2, pp. 139–142, Feb. 2020.
- [24] X. Qiu, T. Jiang, S. Wu, C. Jiang, H. Yao, M. H. Hayes, and A. Benslimane, “Wireless user authentication based on KLT and Gaussian mixture model,” in *Proc. of WCNC*, 2019, pp. 1–5.
- [25] S. Hanna, S. Karunaratne, and D. Cabric, “Open set wireless transmitter authorization: Deep learning approaches and dataset considerations,” *IEEE Trans. Cogn. Commun. Netw.*, vol. 7, no. 1, pp. 59–72, Mar. 2021.
- [26] P. Perera, P. Oza, and V. M. Patel, “One-class classification: A survey,” 2021. [Online]. Available: <https://arxiv.org/abs/2101.03064>
- [27] T. M. Hoang, A. Vahid, H. D. Tuan, and L. Hanzo, “Physical layer authentication and security design in the machine learning era,” *IEEE Commun. Surv. Tutor.*, pp. 1–1, Feb. 2024.
- [28] K. Hempstalk, E. Frank, and I. Witten, “One-class classification by combining density and class probability estimation,” in *Proc. of ECML PKDD*, 2008.
- [29] V. Barnabé-Lortie, C. Bellinger, and N. Japkowicz, “Active learning for one-class classification,” in *Proc. of ICMLA*, 2015, pp. 390–395.
- [30] T. Diskin, U. Okun, and A. Wiesel, “Learning to detect with constant false alarm rate,” in *Proc. of SPAWC*, 2022, pp. 1–5.
- [31] P. Oza and V. M. Patel, “One-class convolutional neural network,” *IEEE Signal Process. Lett.*, vol. 26, no. 2, pp. 277–281, Feb. 2019.
- [32] P. Baracca, N. Laurenti, and S. Tomasin, “Physical layer authentication over MIMO fading wiretap channels,” *IEEE Trans. Wirel. Commun.*, vol. 11, no. 7, pp. 2564–2573, 2012.
- [33] M. Ribeiro, A. E. Lazzaretti, and H. S. Lopes, “A study of deep convolutional auto-encoders for anomaly detection in videos,” *Pattern Recognit. Lett.*, vol. 105, no. C, pp. 13–22, Apr. 2018.
- [34] X. Guo, J. Yang, C. Wu, C. Wang, and Y. Liang, “A novel LS-SVMs hyper-parameter selection based on particle swarm optimization,” *Neurocomputing*, vol. 71, no. 16, pp. 3211–3215, Oct. 2008.
- [35] B. Zhou, C. Han, and T. Guo, “Convergence of stochastic gradient descent in deep neural network,” *Acta Math. Appl. Sin.*, no. 1, pp. 126–136, Jan. 2021.
- [36] M. Ribeiro, M. Gutoski, A. E. Lazzaretti, and H. S. Lopes, “One-class classification in images and videos using a convolutional autoencoder with compact embedding,” *IEEE Access*, vol. 8, pp. 86 520–86 535, May 2020.
- [37] F. Ardizzon, D. Salvaterra, M. Piana, and S. Tomasin, “Energy-based optimization of physical-layer challenge-response authentication with drones,” in *arXiv*, 2024. [Online]. Available: <https://arxiv.org/abs/2405.03608>
- [38] M. Khalid, R. Zhao, and N. Ahmed, “Physical layer authentication in line-of-sight underwater acoustic sensor networks,” in *Proc. of OCEANS*, 2020, pp. 1–5.
- [39] H. Steck and D. G. Garcia, “On the regularization of autoencoders,” 2021. [Online]. Available: <https://arxiv.org/abs/2110.11402>
- [40] T. Hofmann, B. Schölkopf, and A. J. Smola, “Kernel methods in machine learning,” *Ann. Stat.*, vol. 36, no. 3, pp. 1171 – 1220, June 2008.

APPENDIX A  
PROOF OF LEMMA 2

In [35] it is shown that an interactive algorithm satisfying [35, Assumptions 1.2-1.5] with a small enough learning rate converges to the optimal value, according to (29) (see [35, Theorem 3.2]). Assumptions 1.2 and 1.3 pertain only to the loss function,<sup>2</sup> thus if they hold for SGD, they also hold for MSGD. We then focus on the other assumptions.

Assumption 1.4 [35] requires that (28) is an unbiased estimate of the true gradient. Assuming this is true for SGD, we show that it also holds for the modified gradient. In formulas, we must have

$$\mathbb{E}_{\mathcal{D}}[g(\mathbf{q}, t, \mathbf{w})] = \psi \nabla_{\mathbf{w}} \mathbb{E}_{\mathcal{D}}[\beta_{\text{NN}}(\mathbf{q}, t, \mathbf{w})] |_{\mathbf{w}_n}, \quad (42)$$

for some constant  $\psi$ . First, we compute the expectation of the gradient, as (using (28))

$$\mathbb{E}_{\mathcal{D}}[g(\mathbf{q}, t, \mathbf{w}_n)] = \mathbb{E}_{\mathcal{D}_0}[g'(\mathbf{q}, 0, \mathbf{w}_n)] + F(\mathbf{w}_n). \quad (43)$$

<sup>2</sup>Note that loss functions (24) and (23) satisfy Assumptions 1.2 and 1.3.

Then, we compare it with the expectation of the gradient  $g(\mathbf{q}_n, t_n, \mathbf{w}_n)$  of the SGD algorithm with an artificial dataset with the same number of CF vectors as  $\mathcal{D}_0$  (using (26))

$$\begin{aligned}\mathbb{E}[g'(\mathbf{q}, t, \mathbf{w}_n)] &= \sum_{i=1,2} \frac{1}{2} \mathbb{E}_{\mathcal{D}_i}[g'(\mathbf{q}, i, \mathbf{w}_n)] \\ &= \frac{1}{2} \mathbb{E}_{\mathcal{D}_0}[g'(\mathbf{q}, 0, \mathbf{w}_n)] + \frac{1}{2} F(\mathbf{w}_n).\end{aligned}\quad (44)$$

We note that (43) and (44) coincide apart from a scaling factor, thus as by hypothesis (42) (with  $g'$  instead of  $g$ ) is satisfied for the SGD, it is also satisfied for the MSGD.

Similarly, it is possible to verify Assumption 1.5, which requires

$$\frac{\text{Var}_{\mathcal{D}} g(\mathbf{q}, t, \mathbf{w}_n)}{\|g(\mathbf{q}, t, \mathbf{w}_n)\|^2} < M, \quad (45)$$

where

$$\text{Var}_{\mathcal{D}} g(\mathbf{q}, t, \mathbf{w}_n) = \mathbb{E}_{\mathcal{D}} \left[ \|g(\mathbf{q}, t, \mathbf{w}_n) - \mathbb{E}_{\mathcal{D}} [g(\mathbf{q}, t, \mathbf{w}_n)]\|^2 \right]. \quad (46)$$

Indeed, we have

$$\begin{aligned}\frac{\text{Var}_{\mathcal{D}} g(\mathbf{q}, t, \mathbf{w}_n)}{\|g(\mathbf{q}, t, \mathbf{w}_n)\|^2} &= \frac{1}{2} \frac{\text{Var}_{\mathcal{D}_0} g(\mathbf{q}, 0, \mathbf{w}_n)}{\|g(\mathbf{q}, t, \mathbf{w}_n)\|^2} \\ &= \frac{1}{2} \frac{\text{Var}_{\mathcal{D}_0} g'(\mathbf{q}, 0, \mathbf{w}_n)}{\|g'(\mathbf{q}, t, \mathbf{w}_n)\|^2}\end{aligned}\quad (47)$$

where we have exploited the fact that the MSGD operates on a single dataset and that the variance of  $F(\mathbf{w}_n)$  with respect to the data CF vector is zero, i.e.,  $\text{Var}_{\mathcal{D}_1} \hat{g}(\mathbf{q}, 1, \mathbf{w}_n) = 0$ . By the hypothesis, Assumption 1.5 holds for  $g'$  of the SGD algorithm, thus we have

$$\begin{aligned}\frac{\text{Var}_{\mathcal{D}} g(\mathbf{q}, t, \mathbf{w}_n)}{\|g(\mathbf{q}, t, \mathbf{w}_n)\|^2} &= \frac{1}{2} \frac{\text{Var}_{\mathcal{D}_0} g'(\mathbf{q}, 0, \mathbf{w}_n)}{\|g'(\mathbf{q}, t, \mathbf{w}_n)\|^2} + \\ &+ \frac{1}{2} \frac{\text{Var}_{\mathcal{D}_1} g'(\mathbf{q}, 1, \mathbf{w}_n)}{\|g'(\mathbf{q}, t, \mathbf{w}_n)\|^2} < M.\end{aligned}\quad (48)$$

Now, (47) and (48) we immediately obtain (45). Since all the assumptions of [35] hold for the MSGD, we can conclude that it converges to the optimal parameters.

## APPENDIX B PROOF OF THEOREM 3

The aim of this Appendix is to prove Theorem 3. To do so, we first introduce the following Lemma.

**Lemma 3.** *Given a  $\mathbb{R} \rightarrow \mathbb{R}$  invertible function  $h(u)$ , with  $h(u) \geq 0$ ,  $\forall u$ , and  $h(u)$  invertible. Given two models  $\mu_1(\mathbf{x}, \mathbf{w}_1)$  and  $\mu_2(\mathbf{x}, \mathbf{w}_2)$  satisfying*

$$\mu_1(\mathbf{x}, \mathbf{w}_1) = h(\mu_2(\mathbf{x}, \mathbf{w}_2)), \quad (49)$$

*the classifiers obtained using (8) with both models are equivalent.*

*In particular, for any model  $\mu(\mathbf{x}, \mathbf{w})$  satisfying*

$$\mu(\mathbf{x}, \mathbf{w}) = h(p_0(\mathbf{x})), \quad (50)$$

*the resulting test is equivalent to LT.*

*Proof:* From the definition of the decision function (4), we have

$$\begin{aligned}\Delta(\mu_1(\mathbf{x}, \mathbf{w}_1), \delta) &= \begin{cases} \mathcal{H}_0 & \mu_1(\mathbf{x}, \mathbf{w}_1) > \delta \\ \mathcal{H}_1 & \mu_1(\mathbf{x}, \mathbf{w}_1) \leq \delta \end{cases} \\ &= \begin{cases} \mathcal{H}_0 & h(\mu_2(\mathbf{x}, \mathbf{w}_2)) > \delta, \\ \mathcal{H}_1 & h(\mu_2(\mathbf{x}, \mathbf{w}_2)) \leq \delta, \end{cases} \\ &= \begin{cases} \mathcal{H}_0 & \mu_2(\mathbf{x}, \mathbf{w}_2) > h^{-1}(\delta) \\ \mathcal{H}_1 & \mu_2(\mathbf{x}, \mathbf{w}_2) \leq h^{-1}(\delta) \end{cases} \\ &= \Delta(\mu_2(\mathbf{x}, \mathbf{w}_2), h^{-1}(\delta)),\end{aligned}\quad (51)$$

which shows the equivalence of the two classifiers, with suitably selected thresholds. Lastly, when (50) holds, it yields that the classifier with model  $\mu(\mathbf{x}, \mathbf{w})$  has as equivalent decision function  $\Delta(p_0(\mathbf{x}), h^{-1}(\delta))$ , which establishes the equivalence with the LT. ■

We are now ready to prove Theorem 3.

*Proof of Theorem 3:* We consider the modified model  $\bar{\mu}(\mathbf{x}, \mathbf{w}) = \mu(\mathbf{x}, \mathbf{w}) - b$ , which removes the bias term  $b$ , and by Lemma 3 yields an equivalent classifier.

Let  $\bar{\mathbf{x}}_\ell$ ,  $\ell = 1, \dots, L$ , be the distinct vectors of the dataset  $\mathcal{D}_0$ , and let us define the matrix

$$\Phi_0 = [\phi(\bar{\mathbf{x}}_1), \dots, \phi(\bar{\mathbf{x}}_L)]. \quad (52)$$

We assume  $L \geq M$ , i.e., the number of distinct vectors is larger than the number of elements  $\mathbf{x}$ . If  $L < M$  we must expand  $\Phi_0$  by adding  $M - L$  columns orthogonal to the first  $L$  vectors.

Let us consider the change of variable from  $\mathbf{w}$  to  $\bar{\mathbf{w}} = [\bar{w}_1, \dots, \bar{w}_L]^T$ , with

$$\Phi_0^T \mathbf{w} = \bar{\mathbf{w}}. \quad (53)$$

From the orthonormal condition, the system of equations (53) is uniquely solvable, thus we can optimize  $\bar{\mathbf{w}}$  to minimize the loss function, instead of optimizing  $\mathbf{w}$ . To write (12b) as a function of  $\bar{\mathbf{w}}$ , first we note that from (30) we have  $\Phi_0 \Phi_0^T = \mathbf{I}$  the identity matrix, and also

$$\mathbf{w}^T \mathbf{w} = \mathbf{w}^T \Phi_0 \Phi_0^T \mathbf{w} = \sum_{\ell=1}^L \bar{w}_\ell^2. \quad (54)$$

Then, considering an input  $\mathbf{x}$ , the error model correction term from [3] becomes

$$e_n^2 = [b - \mathbf{w}^T \phi(\mathbf{x}_n)]^2, \quad (55)$$

and (12b), becomes

$$\rho_{\text{OLSSVM}}(\mathcal{D}_0, \mathbf{w}, b) = \frac{1}{2} \mathbf{w}^T \mathbf{w} + b + \frac{1}{2} C \sum_{n=1}^{N_0} [b - \mathbf{w}^T \phi(\mathbf{x}_n)]^2. \quad (56)$$

Lastly, from (53) and (55), the objective function becomes (in the new variable  $\bar{\mathbf{w}}$ )

$$\rho_{\text{OLSSVM}}(\mathcal{D}_0, \bar{\mathbf{w}}, b) = \frac{1}{2} \sum_{\ell=1}^L \bar{w}_\ell^2 + b + \frac{1}{2} C \sum_{n=1}^{N_0} [b - \bar{w}_{\ell(n)}]^2, \quad (57)$$

where  $\ell(n)$  is the index of the unique vector corresponding to  $\mathbf{x}_n$ , i.e.,  $\mathbf{x}_n = \bar{\mathbf{x}}_{\ell(n)}$ .

For  $N_0 \rightarrow \infty$ , we can switch from the actual count to probability as,

$$\begin{aligned} \lim_{N_0 \rightarrow \infty} \rho_{\text{OLSSVM}}(\mathcal{D}_0, \bar{\mathbf{w}}, b) &= \\ \frac{1}{2} \sum_{\ell=1}^L \bar{w}_\ell^2 + b + \frac{1}{2} C N_0 \sum_{\ell=1}^L p(\bar{\mathbf{x}}_\ell, \theta_0) [b - \bar{w}_\ell]^2, \end{aligned} \quad (58)$$

and it holds

$$\begin{aligned} \lim_{N_0 \rightarrow \infty} \rho_{\text{OLSSVM}}(\mathcal{D}_0, \bar{\mathbf{w}}, b) &= \\ &= \frac{1}{2} \sum_{\ell=1}^L \bar{w}_\ell^2 + b + \frac{1}{2} C N_0 \sum_{\ell=1}^L p(\bar{\mathbf{x}}_\ell, \theta_0) [b^2 + \bar{w}_\ell^2 - 2b\bar{w}_\ell], \\ &= \frac{1}{2} \sum_{\ell=1}^L \left[ \bar{w}_\ell^2 (1 + C N_0 p(\bar{\mathbf{x}}_\ell, \theta_0)) - 2C N_0 b \bar{w}_\ell p(\bar{\mathbf{x}}_\ell, \theta_0) \right] \\ &\quad + b + \frac{1}{2} C N_0 b^2. \end{aligned} \quad (59)$$

Next, we minimize the loss function over  $\bar{\mathbf{w}}$  by nulling the derivative of the loss function

$$\frac{\partial \rho_{\text{OLSSVM}}(\mathcal{D}_0, \bar{\mathbf{w}}', b)}{\partial \bar{w}'_\ell} = 0, \quad (60)$$

at  $\bar{w}'$ , which yields

$$(1 + C N_0 p(\bar{\mathbf{x}}_\ell, \theta_0)) \bar{w}'_\ell - C N_0 b p(\bar{\mathbf{x}}_\ell, \theta_0) = 0,$$

and

$$\bar{w}'_\ell = \frac{C N_0 b p(\bar{\mathbf{x}}_\ell, \theta_0)}{1 + C N_0 p(\bar{\mathbf{x}}_\ell, \theta_0)}. \quad (61)$$

Lastly, we minimize the loss function over the bias

$$\left. \frac{\partial \rho_{\text{OLSSVM}}(\mathcal{D}_0, \bar{\mathbf{w}}', \bar{b})}{\partial \bar{b}} \right|_{\bar{b}=\tilde{b}} = 0, \quad (62)$$

obtaining

$$\tilde{b} = -\frac{1}{C N_0} + \sum_{\ell=1}^L \bar{w}_\ell p(\bar{\mathbf{x}}_\ell, \theta_0). \quad (63)$$

The resulting model is

$$\bar{\mu}(\mathbf{x}, \mathbf{w}) = \frac{C N_0 \tilde{b} p(\bar{\mathbf{x}}_\ell, \theta_0)}{1 + C N_0 p(\bar{\mathbf{x}}_\ell, \theta_0)}, \quad \text{for } \mathbf{x} = \bar{\mathbf{x}}_\ell. \quad (64)$$

From (64) we conclude that  $\bar{\mu}(\mathbf{x}, \mathbf{w})$  is a monotone non-negative function of  $p_0(\mathbf{x})$  and by Lemma 3 the resulting classifier is equivalent to the LT.

Note that transformation functions of infinite size are typical of SVM, thanks to the kernel trick [40], by which what matters for the model is the kernel  $k(\mathbf{x}, \mathbf{y}) = \bar{\boldsymbol{\phi}}^T(\mathbf{x}) \bar{\boldsymbol{\phi}}(\mathbf{y})$  between CF vectors  $\mathbf{x}$  and  $\mathbf{y}$ .

■